

pubs.acs.org/JACS Article

Expanding the Landscape of Noncanonical Amino Acids in RiPP Biosynthesis

Brooke A. Johnson, Kenzie A. Clark, Leah B. Bushin, Calvin N. Spolar, and Mohammad R. Seyedsayamdost*



Cite This: J. Am. Chem. Soc. 2024, 146, 3805-3815



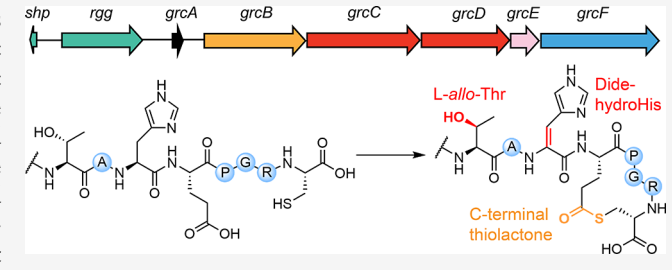
ACCESS I

III Metrics & More

Article Recommendations

s Supporting Information

ABSTRACT: Advancements in DNA sequencing technologies and bioinformatics have enabled the discovery of new metabolic reactions from overlooked microbial species and metagenomic sequences. Using a bioinformatic co-occurrence strategy, we previously generated a network of $\sim\!600$ uncharacterized quorum-sensing-regulated biosynthetic gene clusters that code for ribosomally synthesized and post-translationally modified peptide (RiPP) natural products and are tailored by radical S-adenosylmethionine (RaS) enzymes in streptococci. The most complex of these is the GRC subfamily, named after a conserved



motif in the precursor peptide and found exclusively in *Streptococcus pneumoniae*, the causative agent of bacterial pneumonia. In this study, using both *in vivo* and *in vitro* approaches, we have elucidated the modifications installed by the *grc* biosynthetic enzymes, including a ThiF-like adenylyltransferase/cyclase that generates a C-terminal Glu-to-Cys thiolactone macrocycle, and two RaS enzymes, which selectively epimerize the β -carbon of threonine and desaturate histidine to generate the first instances of L-allo-Thr and didehydrohistidine in RiPP biosynthesis. RaS-RiPPs that have been discovered thus far have stood out for their exotic macrocycles. The product of the *grc* cluster breaks this trend by generating two noncanonical residues rather than an unusual macrocycle in the peptide substrate. These modifications expand the landscape of nonproteinogenic amino acids in RiPP natural product biosynthesis and motivate downstream biocatalytic applications of the corresponding enzymes.

■ INTRODUCTION

The discovery of novel natural product scaffolds has been essential for the creation of pharmaceutical leads and the development of new synthetic reactions. Historically, scientists relied on "grind and find" methods to identify bioactive natural products and possibly new chemical motifs. Unfortunately, over time, these efforts have led to the repeated rediscovery of previously known natural product families and, therefore, diminished focus on what was deemed "genetically gifted" genera. Concurrently, advancements in DNA sequencing technologies and bioinformatic tools at the turn of the century paved the way for targeting microbial species on the basis of the biosynthetic potential written in their genomes. These technologies have facilitated the identification of complex structures from the most unlikely species in a genome-first, rather than an activity-first, approach.

Streptococci provide a representative example. Despite their relatively small genomes of typically <2 Mbp, they can access diverse chemotypes by leveraging the simple biosynthetic logic of ribosomally synthesized and post-translationally modified peptides (RiPPs). RiPP biosynthetic gene clusters (BGCs) typically encode a precursor peptide, which is synthesized by the ribosome, tailoring enzymes, which modify the core region of the peptide, and proteases and

transporters that cleave the leader (and follower) sequence to deliver the mature product into the environment. This biosynthetic framework is found in diverse organisms forming one of the largest classes of natural products and providing bioactive molecules, as well as agriculturally and therapeutically useful metabolites. $^{10-12}$

An intriguing group of RiPPs are those tailored by radical S-adenosylmethionine (RaS) enzymes, a protein superfamily present in all domains of life. $^{13-15}$ RaS enzymes catalyze versatile and complex chemical reactions, including methylations, epimerizations, and notably, an array of macrocyclic C- C and C-heteroatom cross-links at unactivated carbons on peptide substrates. $^{13-17}$ RaS enzymes are united by their radical initiation mechanism. They harbor a [4Fe-4S] cluster in which three of the Fe atoms are held in place by three cysteine residues, while the remaining Fe is coordinated by S-adenosylmethionine (SAM). Reductive homolytic cleavage of

Received: October 1, 2023 Revised: January 14, 2024 Accepted: January 16, 2024

Published: February 5, 2024





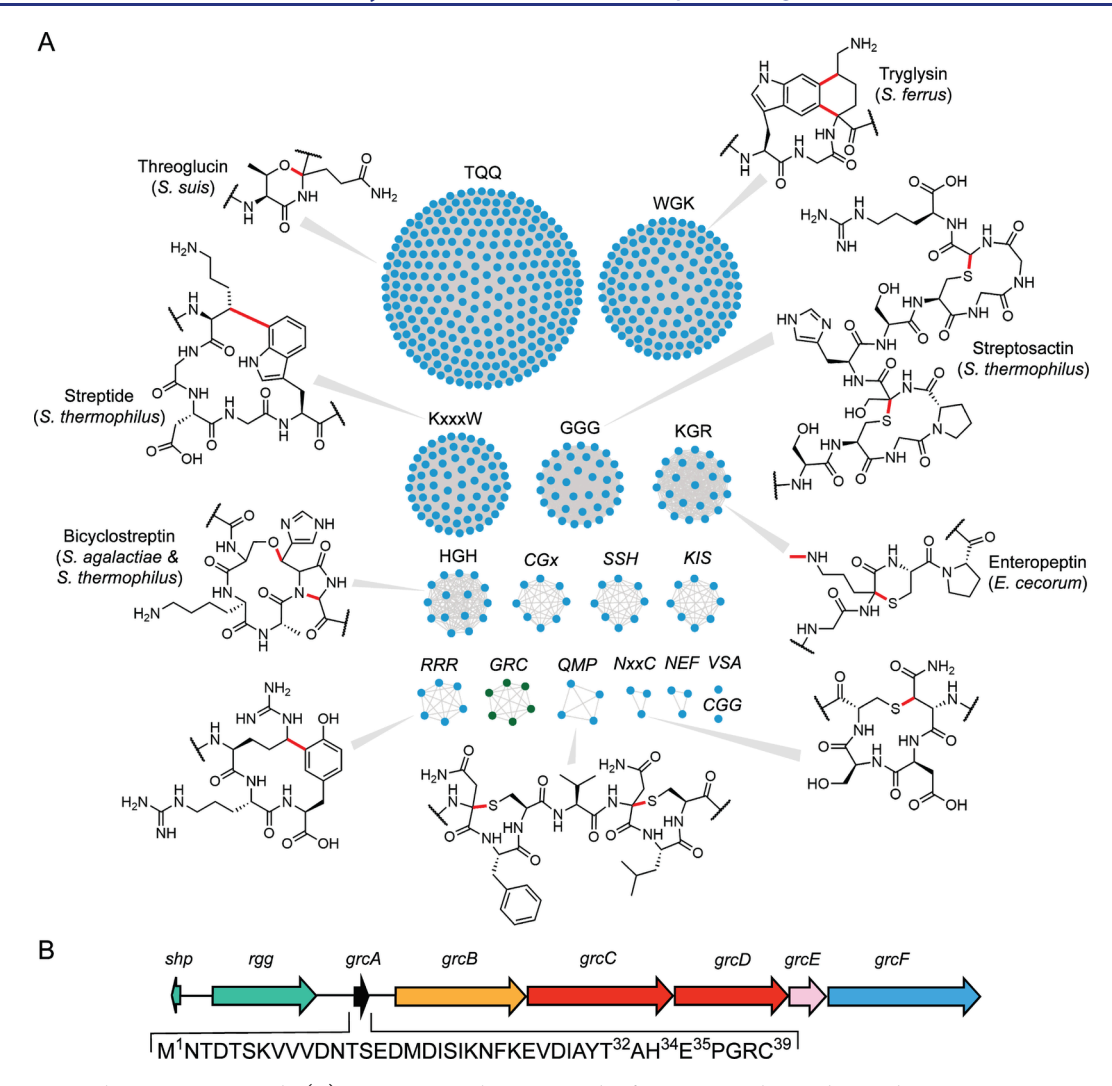


Figure 1. Streptococcal RaS-RiPP network. (A) Sequence similarity network of RaS-RiPPs clustered according to precursor peptide homology, with each node representing an individual BGC. The *GRC* subfamily, the topic of this study, is shown in dark green. Subfamilies are annotated on the basis of conserved residues in the precursor peptide. Those for which a mature product has been isolated are labeled with the compound name and the source organism(s). Bonds installed by RaS and Fe–S-dependent enzymes are highlighted in red. (B) The *grc* gene cluster from *S. pneumoniae* A34562. An *shp/rgg* operon (green) regulates the expression of the cluster that encodes a precursor peptide (GrcA), a putative ThiF-like adenylyltransferase (GrcB), two RaS enzymes (GrcCD), a RiPP recognition element (GrcE), and a transporter (GrcF).

SAM generates a 5'-deoxyadenosyl radical (5'-dA●) that abstracts a H-atom from substrate to start the catalytic cycle. There remain >600 000 uncharacterized RaS enzymes and >15 000 RaS-RiPPs, which is evidence of a yet to be explored chemical and biosynthetic space. ¹⁸

Inspired by the identification of streptide, a RaS-RiPP from *Streptococcus thermophilus* featuring an unusual cross-link between two unactivated carbons in lysine and tryptophan, we sought to uncover additional RaS enzyme-catalyzed peptide modifications from *Streptococcus* spp. ^{19,20} To identify new molecular scaffolds with physiologically relevant activities, our bioinformatics inquiry searched for RaS-RiPP gene clusters adjacent to a quorum sensing (QS) regulation operon. ²¹ About 600 RaS-RiPP BGCs were identified and classified into 16 distinct subfamilies on the basis of precursor peptide homology using sequence similarity networks (Figure 1A). ^{21,22} Since then, we have found almost a dozen new and diverse RaS enzyme-mediated cross-links from bacteria that play important roles in the human microbiome and in health and disease (Figure 1A). ^{23–30}

In this work, we elucidate the modifications installed by the only RaS-RiPP BGC identified in Streptococcus pneumoniae (Figure 1B), an opportunistic pathogen that resides asymptomatically in healthy carriers but is one of the leading causes of pneumonia-based mortality worldwide for immunocompromised individuals.³¹ Only three subfamilies from our network—GRC, SSH, and the recently characterized bicyclostreptins from HGH—contain two RaS enzymes. 22,29 GRC further distinguishes itself by encoding an additional tailoring enzyme, a putative ThiF-like adenylyltransferase, and a RiPP recognition element (RRE), a prevalent protein domain in many RiPP BGCs that has been shown to mediate the interaction of modification enzymes with the precursor peptide.³² Using an in vivo heterologous coexpression platform in which we expressed, purified, and analyzed a series of constructs with different combinations of the grc tailoring enzymes, as well as in vitro enzymatic assays, we decoded the modifications that are introduced onto the precursor peptide, including macrocyclic thiolactone formation, epimerization at a threonine (Thr) β -carbon, and desaturation at a histidine

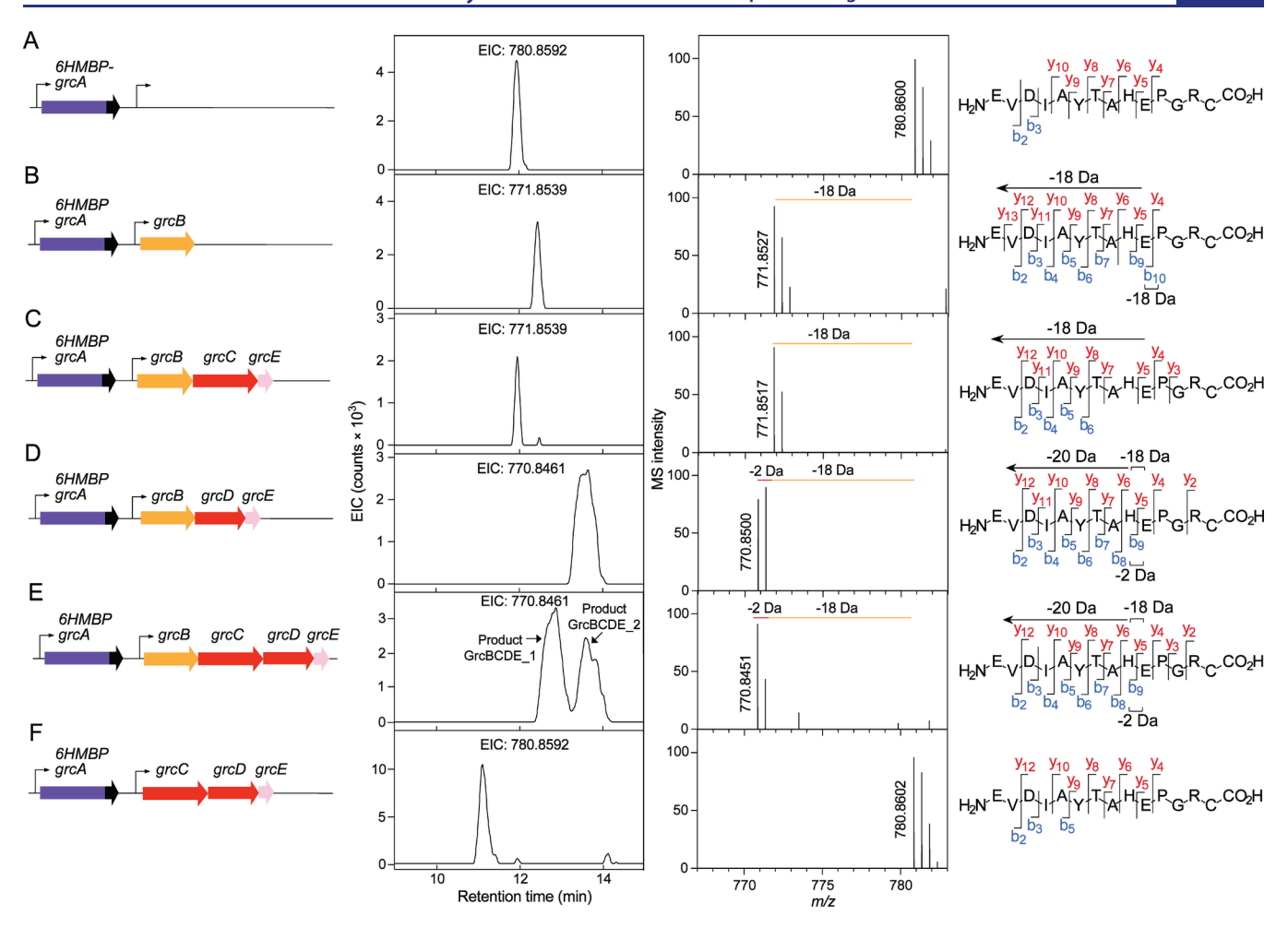


Figure 2. HPLC-coupled HR-MS and HR-MS/MS analysis of heterologous grc coexpression constructs. The plasmid expression construct is depicted on the left followed by an extracted ion chromatogram (EIC, $\Delta ppm = 10 ppm$) and the mass spectrum of the product. The observed HR-MS/MS fragmentation patterns are shown on the right. Note that the mass spectrum is for the $[M + 2H]^{2+}$ ion. Shown are data for GrcA after coexpression with (A) no other enzymes as control, (B) GrcB, (C) GrcBCE, (D) GrcBDE, (E) GrcBCDE, and (F) GrcCDE. Coexpression with GrcB, GrcC, and GrcD gives a -18 Da product, a mass-neutral modification with a slightly shortened retention time, and a -2 Da product, respectively. The chromatograms are focused on the product peaks to highlight chromatographic differences; the column was underloaded in these experiments to facilitate separation of diastereomeric species. No other relevant peaks were observed throughout the elution profile.

(His) residue to generate α,β -didehydro-His, the latter two being novel modifications installed by RaS enzymes. The modified amino acids expand the scope of noncanonical residues that can be incorporated into mature products via the RiPP biosynthetic logic.

RESULTS AND DISCUSSION

GRC Subfamily. In our initial RaS-RiPP streptococcal network, the *GRC* subfamily was unique to *S. pneumoniae* with an identical precursor peptide sequence in all detected *grc* BGCs. In addition to the *shp/rgg* QS operon, the *grc* BGC encodes a 39-mer precursor peptide (GrcA), a putative ThiF-like adenylyltransferase (GrcB), two RaS enzymes (GrcC and GrcD), a discrete RRE protein (GrcE), and a transporter from the major facilitator superfamily (GrcF, Figure 1B).

A heterologous coexpression platform was initially used to determine the modifications installed by the three tailoring enzymes. Starting with a pRSFDuet expression vector, we inserted into the first multiple cloning site *grcA* carrying an N-terminal hexaHis maltose-binding protein (6HMBP) purification tag with an HRV-3C protease cleavage site between the two sequences (Tables S1–S3). In the second multiple cloning

site, we inserted grcB, grcC, grcD, grcE, or a combination of these. Upon expression, modification of the precursor peptide took place within Escherichia coli. Thereafter, the cells were harvested, lysed, and the peptides isolated using immobilized metal affinity chromatography. Finally, the peptides were proteolytically cleaved, and their structures elucidated using high-resolution mass spectrometry (HR-MS), tandem HR-MS (HR-MS/MS), multidimensional nuclear magnetic resonance (NMR) spectroscopy, and Marfey's analysis to determine absolute configurations.

HPLC-Coupled HR-MS and HR-MS/MS Analysis of Enzymatic Products. The *grcA*-only expression construct produced a peptide with the mass of the unmodified, linear precursor, as expected ($[M + 2H]^{2+} = 780.860$, Figure 2A and Tables S4—S6). The construct featuring GrcB, in addition to the precursor peptide, exhibited an 18 Da lighter mass relative to the precursor peptide (Figure 2B). Subsequent cleavage with trypsin localized the modification to the C-terminal 14 residues of the peptide. The -18 Da modification was reflected in the b10 and y5—y13 ions, thereby suggesting either a modified Glu35 or macrocyclization involving Glu35 and one of the downstream residues. Intracross-link ions b10 and y4

suggest that the putative macrocycle can fragment under the spectrometric conditions (Tables S7 and S8). The modification was also observed in the absence of GrcE, which indicated that this standalone RRE was not required for the reaction (Tables S4 and S5). Indeed, further HHpred-based sequence analysis showed that GrcB contains an N-terminal RRE domain. Recombinant constructs that lacked this domain or the C-terminal catalytic domain of GrcB were inactive in generating the -18 Da modification (Figure S1).

Next, we investigated the activity of the RaS enzymes. The peptide product of the GrcBCE construct, in which the first RaS enzyme, GrcC, was present, in addition to GrcB and the RRE GrcE, also gave a -18 Da product with respect to the precursor peptide (Figure 2C and Tables S4-S5). However, this species exhibited different chromatographic properties with a shorter retention time compared with the GrcB-only product (Figure 2C, Table S6). Coinjection of the two products validated this result, which indicated that the two −18 Da products were not identical (Figure S2). In addition, the HR-MS/MS fragmentation pattern for the product of the GrcBCE construct was analogous to those with GrcB alone, consistent with a diastereomeric relationship between the two products (Table S9). Conversely, the GrcBDE product featured a -20 Da mass shift relative to the precursor peptide and an increase in retention time relative to the -18 Da products (Figure 2D). In this product, an observed -18 Da y5 ion, -2 Da b9 ion, and y6-y12 ions with a -20 Da modification relative to GrcA all pointed to a −2 Da modification on His34, as well as the condensation involving Glu35 (Table S10). We also observed the -2 Da modification on His34 without the condensation ascribed to the -18 Da alteration (Tables S11 and S12).

The construct with the full BGC, the putative ThiF-like adenylyltransferase GrcB, both RaS enzymes GrcC and GrcD, and the RRE GrcE gave two -20 Da species relative to the peptide substrate with two different retention times (Figure 2E). We call these species GrcBCDE_1 and GrcBCDE_2, according to their elution profiles. Both species exhibited analogous MS/MS fragmentation patterns; a fragment that was 2 Da lighter localized on His34 and a -18 Da lighter fragment involving Glu35 (Table S13). On the basis of these results, we wondered if one of the -20 Da species was the product of the GrcBDE reaction and, thus, an intermediate. At first glance, the GrcBDE product (Figure 2D) and GrcBCDE 2 (Figure 2E) had identical retention times and HR-MS profiles. When we coinjected GrcBCDE 1 or GrcBCDE 2 with the product from the GrcBDE construct, indeed, the GrcBDE product and GrcBCDE 2 coeluted (Figure 3, Figure S2). Their HR-MS/ MS profiles were very similar, which is consistent with the idea that GrcBCDE 2 is an intermediate and GrcBCDE 1 the final product (Tables S10 and S13). Finally, the GrcCDE construct did not feature the -2 Da modification, thereby suggesting that macrocycle formation preceded and was a requirement for the -2 Da alteration (Table S12). The GrcCDE construct did, however, result in a retention time shift, which suggests that the mass-neutral modification can occur on the linear precursor (Figure S2).

As a final experiment with the *in vivo* constructs, we explored the importance of the recognizable, discrete RRE protein (GrcE). We found that GrcB and GrcC do not require this domain because their reactions occurred in the absence of GrcE (Tables S4-S6). However, the -2 Da modification was

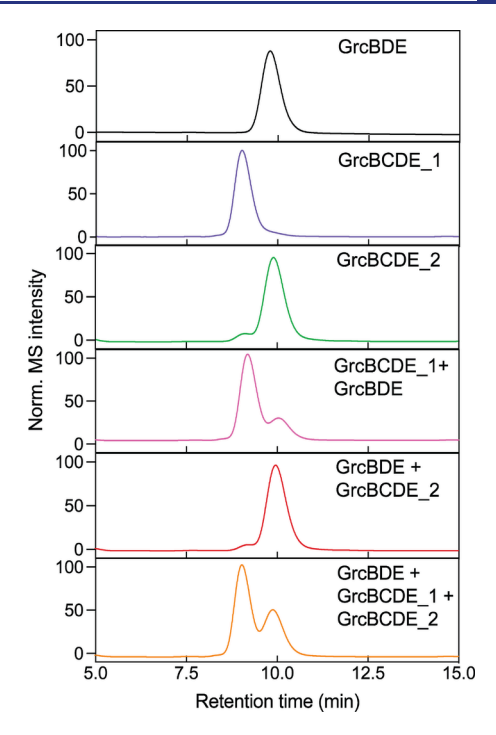


Figure 3. HPLC-MS coinjection data for the -20 Da products GrcBCDE_1, GrcBCDE_2, and GrcBDE. Shown are EIC traces (m/z = 770.8461, Δ ppm = 10). The GrcBDE and GrcBCDE_2 products both have longer retention times relative to GrcBCDE_1 and coelute. Together with identical HR-MS/MS patterns, these data indicate that GrcBDE and GrcBCDE_2 are intermediates in the pathway. The GrcBCDE_1 product does not coelute with the other species, which suggests it contains a mass-neutral alteration.

not observed unless GrcE was present, which suggests it is required for the GrcD-catalyzed transformation.

Structural Elucidation of the GrcBCDE Products by NMR. To definitively determine the structure of the species above, we conducted large-scale growth and purification of the two -20 Da products from expression of GrcBCDE and GrcBDE and subjected these to a suite of multidimensional NMR experiments (Table S14, Figures S3-S5). The linear unmodified GrcA 14-mer peptide was obtained commercially for comparison. ¹H, COSY, and heteronuclear multiple bond correlation (HMBC) spectra of the GrcBDE product revealed chemical shift changes at the Glu35 and Cys39 side-chains relative to the linear peptide. Both the γ -protons of Glu35 and the β -protons of Cys39 strongly correlated to a carbonyl group with a ¹³C shift at 201.4 ppm (Figure 4A). This significant downfield shift and other correlations are consistent with a thioester linkage between Glu35 and Cys39. Low isolation yields and signal-to-noise precluded detection of this shift in the HMBC spectrum of the final GrcBCDE 1-modified product. However, on the basis of the overlap between NMR features and analogous shifts throughout, in addition to the HR-MS/MS data, we assign the -18 Da transformation to installation of a thiolactone, catalyzed by GrcB in both GrcBDE and GrcBCDE products. Thioester linkages are more easily fragmented than their amide or ester counterparts, which is consistent with the MS/MS fragments that are detected within the Glu-to-Cys cross-link (Figure 2).

Next, we turned to the distinct proton shift in the midaromatic region (around 7.6 ppm) present in the H^1 NMR spectra of both the intermediate (GrcBDE and

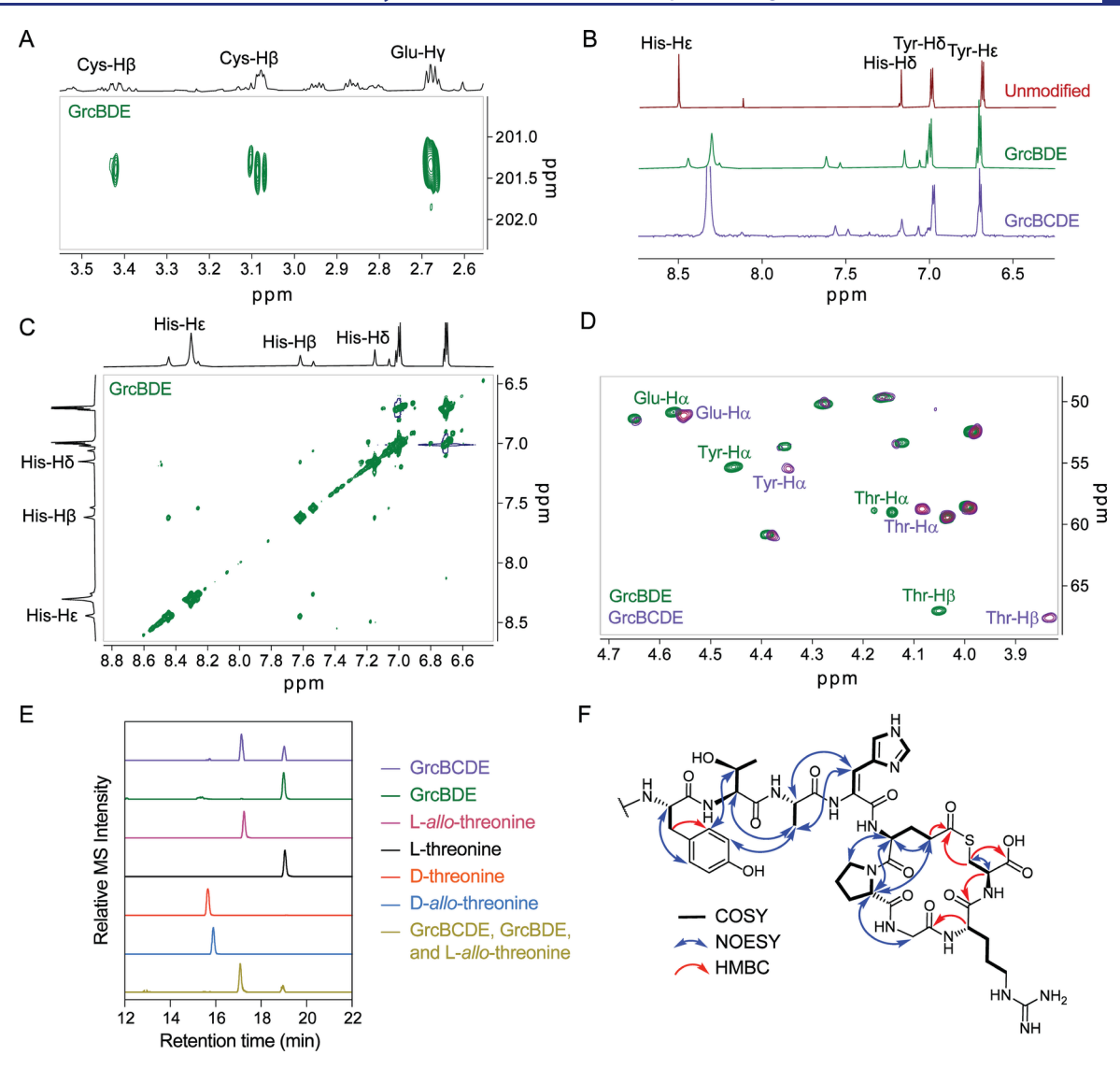


Figure 4. Structural elucidation of GrcBCDE- and GrcBDE-modified peptides. (A) HMBC spectrum of GrcBDE reveals thioester linkage connecting Glu and Cys. (B) Stacked 1 H NMR of unmodified standard, GrcBDE, and GrcBCDE products shows a new peak in the aromatic region around 7.6 ppm. Note that the 1 H signals appear as twinned peaks in unequal ratios only upon macrocycle formation; this likely occurs as a result of conformational isomerism. (C) COSY spectrum of GrcBDE shows that this 7.6 ppm peak correlates with the δ and the ε protons of His34 and is indicative of histidine didehydrogenation. (D) Heteronuclear single quantum coherence (HSQC) overlay of the GrcBDE and GrcBCDE products suggests GrcC epimerizes Thr or tyrosine (Tyr). (E) Marfey's analysis of GrcBDE and GrcBCDE product indicates the presence of L-allo-Thr in the final product. Shown are EIC traces for threonine—Marfey's reagent adduct ([M + H] $^+$ = 372.1150, Δppm = 10). The order of traces matches that in the legend from top to bottom. (F) Structure of the GrcBCDE final product with key correlations annotated.

GrcBCDE 2) and the final product (GrcBCDE 1) but not in the substrate (Figure 4B). The 7.6 ppm shift was correlated with the δ - and the ε -protons of His34 by COSY-NMR, which was consistent with the HR-MS/MS results that localized the modification onto this His residue (Figure 4C). In addition, the expected COSY correlations between the α - and β -protons of His34 were absent in GrcBDE and both GrcBCDE-modified peptides (Figures S3-S5). These results, along with the presence of NOESY correlations between the 7.6 ppm shift and the α - and β -protons of Ala33, were indicative of an α , β unsaturated His residue, a conclusion that is consistent with the broadened absorption spectrum of the product relative to the substrate (Figure S6). Moreover, NOESY correlations observed between the δ -proton of His34 and both the Glu N– H and the β -proton of His34 revealed a *trans*-configuration of the α,β -didehydroHis in addition to the presence of

correlations between the β -proton of His and the α - and β -protons of Ala33 (Figure S7). Thus, GrcD dehydrogenates His34 in a *trans*-selective fashion to generate the olefin product.

To distinguish between the intermediate (GrcBDE-modified peptide) and the final product (GrcBCDE-modified), we overlaid the HSQC spectra of both species and observed chemical shift differences in the Thr32 α - and β -protons and Tyr31 α -protons (Figure 4D). The chemical shifts were most dramatic for the Thr32 β -protons, which were shifted upfield from 4.06 to 3.83 ppm in the product (Table S14). Since GrcC was shown to catalyze a mass-neutral modification on the basis of our HR-MS data, we turned to Marfey's analysis to determine the absolute configuration of the intermediate and the mature product.³³ After functionalizing the hydrolyzed peptides with Marfey's reagent, we determined that all amino

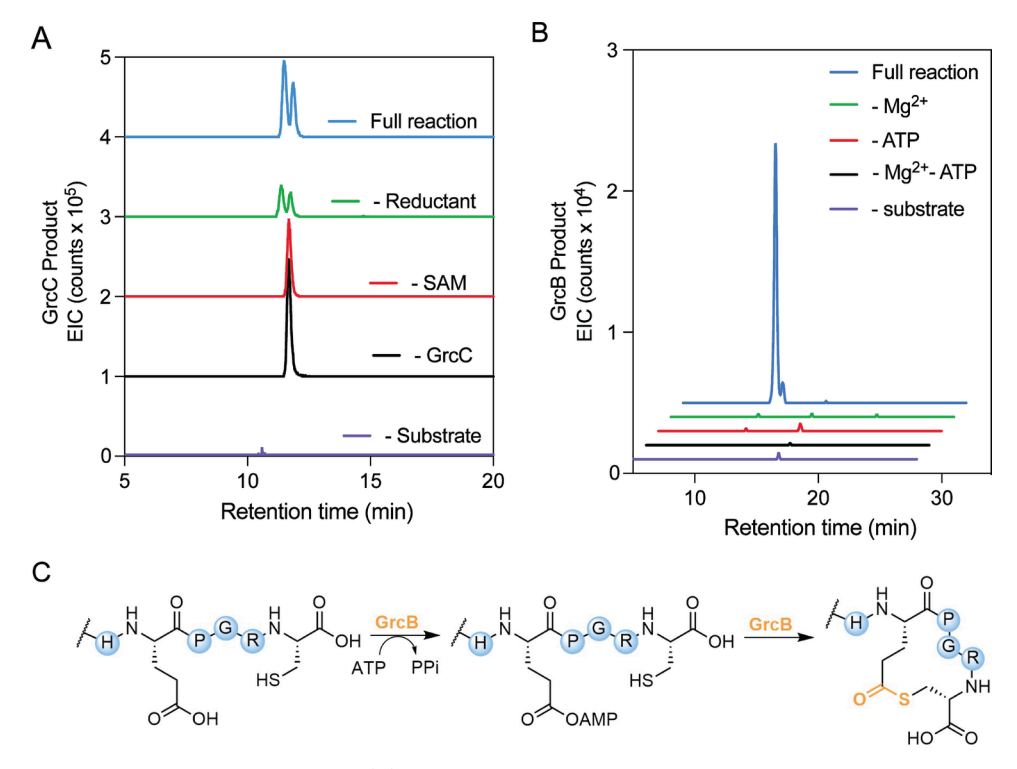


Figure 5. Characterizations of GrcC and GrcB in vitro. (A) Enzymatic activity of GrcC in vitro via HPLC-QTOF-MS analysis. Shown are EIC traces for the GrcC mass neutral product $(m/z = 780.8592, \Delta ppm = 10)$. The product peak is the leftmost peak and is only present if SAM and enzyme are present. (B) Enzymatic activity of GrcB in vitro with GrcC product as a substrate. Shown are EIC traces for the GrcB product $(m/z = 771.8539, \Delta ppm = 10)$. GrcB is only active in the presence of Mg²⁺ and ATP. (C) Proposed reaction scheme for GrcB.

acids in the GrcBDE-modified peptide are L-configured (Figure S8). However, the Thr in the GrcBCDE product displayed an identical retention time to L-allo-Thr, thereby indicating that it is epimerized at the β -carbon (Figure 4E).

Taken together, both GrcBDE- and GrcBCDE-modified peptides possess a thioester linkage between Glu35 and Cys39 and a didehydrohistidine installed by GrcB and GrcDE, respectively. In addition, the final product contains an L-allo-Thr32 epimerized by GrcC (Figure 4F). The macrocyclic proline, which is strictly conserved in GrcA, was found in a *trans*-configuration, as shown by NOESY correlations. On the basis of these findings, we envision a reaction scheme where either GrcB or GrcC install the modification first onto the precursor peptide to generate a macrocyclic thioester and an epimerized Thr32. These are followed by GrcDE, which oxidize His34 to generate an α,β -unsaturated residue. Thus, the three enzymes install novel and an unusual set of modifications onto the core sequence of GrcA.

Reconstitution of the GrcC and GrcB Reactions *In Vitro.* After elucidating the enzymatic reactions *in vivo*, we sought to reconstitute the activity of the enzymes *in vitro* and to reassess the order of the reactions. GrcC, GrcB, and GrcD were cloned into a pET-28b vector with an N-terminal hexahistidine tag. Repeated attempts to obtain soluble GrcD failed, even though the protein was soluble and functional in our *in vivo* studies. This is a common phenomenon with biosynthetic enzymes for which suitable *ex vivo* conditions cannot be easily identified. We were, however, able to purify GrcB and GrcC and conduct *in vitro* enzymatic assays. The *in vivo* experiments showed that the unmodified peptide is accepted by GrcC and GrcB but not GrcD, which suggests that GrcD acts last in the pathway (Tables S4—S6). Therefore, HRV-3C-cleaved GrcA peptide was also expressed, purified,

and used as the substrate in the reactions. The UV–vis absorption spectrum of as-isolated GrcC was characteristic of a RaS enzyme exhibiting a broad band at 400 nm and a shoulder around \sim 320 nm (Figure S9). Quantification of Fe and labile S²- gave 5.5 \pm 0.1 Fe and 6.0 \pm 0.1 S²- per protomer, which is consistent with the presence of at least two [4Fe–4S] clusters. In the absence of substrate, GrcC was able to convert SAM into 5′-deoxyadenosine, thereby indicating it can trigger the radical initiation reaction that is characteristic of the RaS enzyme family (Figure S9).

We next supplemented the GrcC reaction with GrcA, reductant, and SAM. After defined intervals, the enzyme was removed, and the peptides were subjected to tryptic digestion followed by HPLC-MS analysis. When all reaction components were present, we observed a new peak consistent with a mass neutral modification, as shown by HR-MS and HR-MS/MS analysis (Figure 5A, Tables S15 and S16). This peak was not formed in the absence of SAM or GrcC and accumulated in a time-dependent manner (Figure S10, Figure 5A). Moreover, when GrcA was replaced with the product of the GrcB reaction—that is, GrcA containing the C-terminal thiolactone macrocycle—significant product formation was not detected (Figure S11). Together, these data show that GrcC can catalyze Thr β -carbon epimerization *in vitro* and that the enzyme prefers the linear GrcA substrate.

The RaS epimerase YydG inverts the α -carbon configuration of valine and isoleucine residues in its precursor peptide via 5′-dA•-mediated abstraction of α -protons followed by H-atom donation from the other face of the resulting radical intermediate. A Cys residue in YydG has been identified as the H-atom donor. Interestingly, a similar mechanism has been proposed for RaS epimerases that act on glycosidic substrates in hygromycin biosynthesis. To explore the GrcC

Figure 6. Reactions catalyzed by enzymes in the *grc* gene cluster. GrcC catalyzes epimerization at the Thr β -carbon to generate L-allo-Thr. GrcB then condenses the C-terminal Cys with the internal Glu side chain to generate a macrocyclic thiolactone. Finally, GrcDE catalyzes dehydrogenation to give rise to an α , β -didehydroHis residue.

reaction further, we carried out the reaction in fully deuterated buffer. Under these conditions, we observed formation of a product that was 1 Da heavier relative to reaction product in protonated buffer (Figure S12, Table S15). Moreover, HR-MS/MS analysis showed that the mass increase was associated solely with Thr32 in GrcA (Figure S12, Table S17). These results are in line with those observed for YydG and provide a starting point for future mechanistic studies.

ThiF-like adenylyltransferases derive their name from thiamine biosynthesis and require Mg²⁺ and ATP for activity. To reconstitute the activity of GrcB *in vitro*, GrcB was supplemented with Mg²⁺ and ATP in the presence of unmodified or epimerized substrate. Product was observed only when both ATP and Mg²⁺ were present in a time-dependent manner, as determined by HR-MS and HR-MS/MS (Figure 5B, Figure S13). Although GrcB was active on both substrates, the enzyme exhibited a slight preference for the GrcC-epimerized product (Figure S14 and Tables S15, S18, and S19). We could, therefore, recapitulate the reaction of GrcB *in vitro* and gain further insights into the order of reactions of the three modification enzymes in the *grc* BGC (Figure 5C).

CONCLUSION

The identification of GrcC as a Thr β -carbon epimerase adds a new modification to the repertoire of RaS enzymes. Epipeptides and proteusins are classes of RaS-RiPPs that contain valine, isoleucine, and phenylalanines that are epimerized at the α -carbon by the RaS enzymes YydG (an epipeptide epimerase) and by PlpD, OspD, and AvpD (proteusin epimerases). $^{36,37,41-48}$ In the case of the highly cytotoxic polytheonamides, $^{49-51}$ which features a number of post-translational modifications, the RaS enzyme PoyD epimerizes an impressive 18 amino acids, including valine, alanine, asparagine, serine, and Thr, on one 48-mer peptide substrate. Nonetheless, each of these modifications has been limited to the α -carbon, thus giving rise to D-allo-Thr in the case of the Thr modification. Finally, cypemicin is a linaridin-type RiPP that contains D-allo-isoleucine, though epimerization is not carried out by a RaS enzyme. $^{52-57}$ To the best of our knowledge, GrcC distinguishes itself from

previously characterized RaS epimerases in that it acts on the β -carbon instead of the backbone. While L-allo-Thr has been observed in natural products derived from nonribosomal peptide synthetases, such as lysobactin, astin, and globomycin, the noncanonical residue in these cases is thought to be introduced by a heterolytic pathway. S8-60

The characterization of GrcB as an enzyme that introduces a thioester linkage between an internal Glu side chain and a Cterminal Cys also adds a new reaction to the growing list catalyzed by the ThiF/E1-enzyme superfamily.⁶¹ Analysis of the genetic sequence using HHpred revealed that GrcB is bimodal, in that it contains both an N-terminal RRE domain and a C-terminal catalytic domain, and is structurally homologous to the previously characterized proteins MccB and PaaA, which are involved in Asn and Glu-Glu cyclization reactions, respectively. 62,63 The product of the GrcB reaction is reminiscent of the five-residue thiolactone macrocycles found in autoinducing peptides (AIPs) from Staphylococcus aureus but distinct in that its directionality is reversed: in AIPs, an internal Cys reacts with the C-terminal carboxylic acid, whereas the product of GrcB links an internal Glu side chain with a C-terminal Cys-thiol. 64-66 AIPs play important roles in QS and intraspecies communication, which is an intriguing parallel given that the grc BGC is also regulated by QS and that preliminary studies of mature streptococcal RaS-RiPPs suggest that these peptides show fratricidal activities.9

The GrcD-catalyzed dehydrogenation of His is only observed after thiolactone formation and in the presence of the RRE GrcE. Lanthionines are a defining feature of lanthipeptides, with 2,3-didehydroalanine or (Z)-2,3-didehydrobutyrine serving as intermediates toward thioether crosslinks or as residues in the mature RiPP. ^{11,12,67} By leveraging radical chemistry, GrcD expands the scope of α , β -didehydroamino acids in RiPP biosynthesis beyond dehydroalanine and dehydrobutyrine. The RaS maturase, MftC, from the biosynthetic pathway of the redox cofactor mycofactocin decarboxylates the C-terminal tyrosine of the precursor to generate an α , β -dehydrogenated tyramine intermediate, which after reduction of the active site Fe–S cluster by the SPASM domain reacts further with the peptide backbone to form a C–C cross-link. ^{68,69} With only four total Cys residues, GrcD likely

only contains a single [4Fe-4S] cluster in its active site and, unlike MftC, does not react further, thus installing the first instance of dehydrogenated His onto its substrate.

The *in vivo* and *in vitro* studies allow us to propose an order for these modifications wherein GrcC likely acts first to epimerize the Thr32 β -carbon followed by macrocyclization via a C-terminal thiolactone by GrcB and, finally, dehydrogenation of His34 by GrcDE (Figure 6). The product of the *grc* cluster consists of a mosaic of seemingly unrelated modifications reminiscent of the linaridin class of RiPPs. ^{12,52–57} Cypemicin, the founding member of the linaridins mentioned above, features a C-terminal cross-link involving Cys and several dehydroamino acids in addition to epimerized residues, which are not introduced by a RaS enzyme. It will be interesting to uncover how the various modifications in the mature *grc* product contribute to its biological activity.

The two new nonproteinogenic residues introduced by RaS enzymes underscore the rich potential of RiPP BGCs as sources of unusual amino acid alterations. RaS-RiPPs have thus far stood out for their unusual macrocycles. 21-30,70-80 With three modifications and no RaS enzyme-mediated macrocycle, the product of the grc cluster represents one of the most distinct structures in our network. The low abundance of natural products often makes their discovery challenging. However, robust in vivo heterologous expression technologies enable discovery of new scaffolds and post-translational modifications, as they did in this study, by decoding the biosynthetic potential written in microbial genomes. Knowledge of the reactions carried out by GrcBCDE provides important clues in searching for the mature product. Initial efforts to identify the mature RiPP from the grc BGC in S. pneumoniae A34562 were unsuccessful. However, dozens of other S. pneumoniae strains remain to be analyzed. Future efforts to find the mature RiPP will also focus on Streptococcus oralis, an additional species that was sequenced and shown to possess the grc gene cluster after the initial generation of our RaS-RiPP network. Macrococcus caseolyticus, an opportunistic pathogen isolated from dairy products, offers an alternative strain as it encodes a homologous grc cluster on a plasmid, albeit with a different precursor peptide sequence.⁸¹ These strains further underline the complex secondary metabolites that are encoded in underexplored microbes, notably those with small genomes.

ASSOCIATED CONTENT

Supporting Information

The Supporting Information is available free of charge at https://pubs.acs.org/doi/10.1021/jacs.3c10824.

Detailed materials and methods, tabulated HR-MS and HR-MS/MS data for all products reported, 1D/2D NMR spectra, and results of Marfey's analysis (PDF)

AUTHOR INFORMATION

Corresponding Author

Mohammad R. Seyedsayamdost — Department of Chemistry, Princeton University, Princeton, New Jersey 08544, United States; Department of Molecular Biology, Princeton University, Princeton, New Jersey 08544, United States; orcid.org/0000-0003-2707-4854; Email: mrseyed@princeton.edu

Authors

Brooke A. Johnson — Department of Chemistry, Princeton University, Princeton, New Jersey 08544, United States; orcid.org/0009-0000-4575-6467

Kenzie A. Clark — Department of Chemistry, Princeton University, Princeton, New Jersey 08544, United States Leah B. Bushin — Department of Chemistry, Princeton University, Princeton, New Jersey 08544, United States; orcid.org/0000-0003-0538-2469

Calvin N. Spolar – Department of Chemistry, Princeton University, Princeton, New Jersey 08544, United States

Complete contact information is available at: https://pubs.acs.org/10.1021/jacs.3c10824

Funding

We thank the Edward C. Taylor 3rd Year Fellowship in Chemistry (to B.A.J. and C.N.S.), the Eli Lilly Edward C. Taylor Fellowship in Chemistry (to K.A.C.), the National Science Foundation (NSF GRFP to L.B.B. and CAREER Award 1847932 to M.R.S.), and the National Institutes of Health (grant GM129496 to M.R.S.) for financial support.

Notes

The authors declare no competing financial interest.

ACKNOWLEDGMENTS

We thank István Pelczer for technical support with NMR spectra and Chase Kayrouz for helpful conversations.

REFERENCES

- (1) Clardy, J.; Walsh, C. Lessons from Natural Molecules. *Nature* **2004**, 432, 829–837.
- (2) Demain, A. L.; Sanchez, S. Microbial Drug Discovery: 80 Years of Progress. J. Antibiot. 2009, 62, 5–16.
- (3) Newman, D. J.; Cragg, G. M. Natural Products as Sources of New Drugs over the Nearly Four Decades from 01/1981 to 09/2019. *J. Nat. Prod.* **2020**, 83, 770–803.
- (4) Miller, S. J.; Clardy, J. Natural Products: Beyond Grind and Find. *Nat. Chem.* **2009**, *1*, 261–263.
- (5) Baltz, R. H. Gifted Microbes for Genome Mining and Natural Product Discovery. J. Ind. Microbiol. Biotechnol. 2017, 44, 573-588.
- (6) Bachmann, B. O.; Van Lanen, S. G.; Baltz, R. H. Microbial Genome Mining for Accelerated Natural Products Discovery: Is a Renaissance in the Making? *J. Ind. Microbiol. Biotechnol.* **2014**, 41, 175–184.
- (7) Katz, L.; Baltz, R. H. Natural Product Discovery: Past, Present, and Future. *J. Ind. Microbiol. Biotechnol.* **2016**, 43, 155–176.
- (8) Scott, T. A.; Piel, J. The Hidden Enzymology of Bacterial Natural Product Biosynthesis. *Nat. Rev. Chem.* **2019**, *3*, 404–425.
- (9) Clark, K. A.; Bushin, L. B.; Seyedsayamdost, M. R. RaS-RiPPs in Streptococci and the Human Microbiome. *ACS Bio. Med. Chem. Au* **2022**, *2*, 328–339.
- (10) Arnison, P. G.; Bibb, M. J.; Bierbaum, G.; Bowers, A. A.; Bugni, T. S.; Bulaj, G.; Camarero, J. A.; Campopiano, D. J.; Challis, G. L.; Clardy, J.; Cotter, P. D.; Craik, D. J.; Dawson, M.; Dittmann, E.; Donadio, S.; Dorrestein, P. C.; Entian, K.-D.; Fischbach, M. A.; Garavelli, J. S.; Göransson, U.; Gruber, C. W.; Haft, D. H.; Hemscheidt, T. K.; Hertweck, C.; Hill, C.; Horswill, A. R.; Jaspars, M.; Kelly, W. L.; Klinman, J. P.; Kuipers, O. P.; Link, A. J.; Liu, W.; Marahiel, M. A.; Mitchell, D. A.; Moll, G. N.; Moore, B. S.; Müller, R.; Nair, S. K.; Nes, I. F.; Norris, G. E.; Olivera, B. M.; Onaka, H.; Patchett, M. L.; Piel, J.; Reaney, M. J. T.; Rebuffat, S.; Ross, R. P.; Sahl, H.-G.; Schmidt, E. W.; Selsted, M. E.; Severinov, K.; Shen, B.; Sivonen, K.; Smith, L.; Stein, T.; Süssmuth, R. D.; Tagg, J. R.; Tang, G.-L.; Truman, A. W.; Vederas, J. C.; Walsh, C. T.; Walton, J. D.; Wenzel, S. C.; Willey, J. M.; van der Donk, W. A. Ribosomally

- Synthesized and Post-Translationally Modified Peptide Natural Products: Overview and Recommendations for a Universal Nomenclature. *Nat. Prod. Rep.* **2013**, *30*, 108–160.
- (11) Ortega, M. A.; van der Donk, W. A. New Insights into the Biosynthetic Logic of Ribosomally Synthesized and Post-Translationally Modified Peptide Natural Products. *Cell Chem. Biol.* **2016**, 23, 31–44.
- (12) Montalbán-López, M.; Scott, T. A.; Ramesh, S.; Rahman, I. R.; van Heel, A. J.; Viel, J. H.; Bandarian, V.; Dittmann, E.; Genilloud, O.; Goto, Y.; Grande Burgos, M. J.; Hill, C.; Kim, S.; Koehnke, J.; Latham, J. A.; Link, A. J.; Martínez, B.; Nair, S. K.; Nicolet, Y.; Rebuffat, S.; Sahl, H.-G.; Sareen, D.; Schmidt, E. W.; Schmitt, L.; Severinov, K.; Süssmuth, R. D.; Truman, A. W.; Wang, H.; Weng, J.-K.; van Wezel, G. P.; Zhang, Q.; Zhong, J.; Piel, J.; Mitchell, D. A.; Kuipers, O. P.; van der Donk, W. A. New Developments in RiPP Discovery, Enzymology and Engineering. *Nat. Prod. Rep.* **2021**, 38, 130–239.
- (13) Frey, P. A.; Hegeman, A. D.; Ruzicka, F. J. The Radical SAM Superfamily. *Crit. Rev. Biochem. Mol. Biol.* **2008**, 43, 63–88.
- (14) Booker, S. J. Anaerobic Functionalization of Unactivated C-H Bonds. *Curr. Opin. Chem. Biol.* **2009**, *13*, 58–73.
- (15) Broderick, J. B.; Duffus, B. R.; Duschene, K. S.; Shepard, E. M. Radical S-Adenosylmethionine Enzymes. *Chem. Rev.* **2014**, *114*, 4229–4317.
- (16) Latham, J. A.; Barr, I.; Klinman, J. P. At the Confluence of Ribosomally Synthesized Peptide Modification and Radical S-Adenosylmethionine (SAM) Enzymology. *J. Biol. Chem.* **2017**, 292, 16397–16405.
- (17) Mahanta, N.; Hudson, G. A.; Mitchell, D. A. Radical Sadenosylmethionine Enzymes Involved in RiPP Biosynthesis. *Biochemistry* **2017**, *56*, 5229–5244.
- (18) Clark, K. A.; Seyedsayamdost, M. R. Bioinformatic Atlas of Radical SAM Enzyme-Modified RiPP Natural Products Reveals an Isoleucine—Tryptophan Crosslink. *J. Am. Chem. Soc.* **2022**, *144*, 17876—17888.
- (19) Ibrahim, M.; Guillot, A.; Wessner, F.; Algaron, F.; Besset, C.; Courtin, P.; Gardan, R.; Monnet, V. Control of the Transcription of a Short Gene Encoding a Cyclic Peptide in *Streptococcus thermophilus*: A New Quorum-Sensing System? *J. Bacteriol.* **2007**, *189*, 8844–8854.
- (20) Schramma, K. R.; Bushin, L. B.; Seyedsayamdost, M. R. Structure and Biosynthesis of a Macrocyclic Peptide Containing an Unprecedented Lysine-to-Tryptophan Crosslink. *Nat. Chem.* **2015**, *7*, 431–437.
- (21) Bushin, L. B.; Clark, K. A.; Pelczer, I.; Seyedsayamdost, M. R. Charting an Unexplored Streptococcal Biosynthetic Landscape Reveals a Unique Peptide Cyclization Motif. *J. Am. Chem. Soc.* **2018**, *140*, 17674–17684.
- (22) Oberg, N.; Precord, T. W.; Mitchell, D. A.; Gerlt, J. A. RadicalSAM.org: A Resource to Interpret Sequence-Function Space and Discover New Radical SAM Enzyme Chemistry. *ACS Bio. Med. Chem. Au* **2022**, *2*, 22–35.
- (23) Caruso, A.; Bushin, L. B.; Clark, K. A.; Martinie, R. J.; Seyedsayamdost, M. R. Radical Approach to Enzymatic β -Thioether Bond Formation. *J. Am. Chem. Soc.* **2019**, *141*, 990–997.
- (24) Clark, K. A.; Bushin, L. B.; Seyedsayamdost, M. R. Aliphatic Ether Bond Formation Expands the Scope of Radical SAM Enzymes in Natural Product Biosynthesis. *J. Am. Chem. Soc.* **2019**, *141*, 10610–10615.
- (25) Caruso, A.; Martinie, R. J.; Bushin, L. B.; Seyedsayamdost, M. R. Macrocyclization via an Arginine-Tyrosine Crosslink Broadens the Reaction Scope of Radical S-Adenosyl-methionine Enzymes. *J. Am. Chem. Soc.* **2019**, *141*, 16610–16614.
- (26) Bushin, L. B.; Covington, B. C.; Rued, B. E.; Federle, M. J.; Seyedsayamdost, M. R. Discovery and Biosynthesis of Streptosactin, a Sactipeptide with an Alternative Topology Encoded by Commensal Bacteria in the Human Microbiome. *J. Am. Chem. Soc.* **2020**, *142*, 16265–16275.
- (27) Caruso, A.; Seyedsayamdost, M. R. Radical SAM Enzyme QmpB Installs Two 9-Membered Ring Sactionine Macrocycles during

- Biogenesis of a Ribosomal Peptide Natural Product. J. Org. Chem. 2021, 86, 11284–11289.
- (28) Rued, B. E.; Covington, B. C.; Bushin, L. B.; Szewczyk, G.; Laczkovich, I.; Seyedsayamdost, M. R.; Federle, M. J. Quorum Sensing in *Streptococcus mutans* Regulates Production of Tryglysin, a Novel RaS-RiPP Antimicrobial Compound. *mBio* **2021**, *12*, e02688-20.
- (29) Bushin, L. B.; Covington, B. C.; Clark, K. A.; Caruso, A.; Seyedsayamdost, M. R. Bicyclostreptins Are Radical SAM Enzyme-Modified Peptides with Unique Cyclization Motifs. *Nat. Chem. Biol.* **2022**, *18*, 1135–1143.
- (30) Clark, K. A.; Covington, B. C.; Seyedsayamdost, M. R. Biosynthesis-Guided Discovery Reveals Enteropeptins as Alternative Sactipeptides Containing N-Methylornithine. *Nat. Chem.* **2022**, *14*, 1390–1398.
- (31) Weiser, J. N.; Ferreira, D. M.; Paton, J. C. Streptococcus pneumoniae: Transmission, Colonization and Invasion. Nat. Rev. Microbiol. 2018, 16, 355–367.
- (32) Burkhart, B. J.; Hudson, G. A.; Dunbar, K. L.; Mitchell, D. A. A Prevalent Peptide-binding Domain Guides Ribosomal Natural product Biosynthesis. *Nat. Chem. Biol.* **2015**, *11*, 564–570.
- (33) Bhushan, R.; Brückner, H. Marfey's Reagent for Chiral Amino Acid Analysis: A Review. *Amino Acids* **2004**, *27*, 231–47.
- (34) Nam, H.; An, J. S.; Lee, J.; Yun, Y.; Lee, H.; Park, H.; Jung, Y.; Oh, K. B.; Oh, D. C.; Kim, S. Exploring the Diverse Landscape of Biaryl-Containing Peptides Generated by Cytochrome P450 Macrocyclases. *J. Am. Chem. Soc.* **2023**, *145*, 22047–22057.
- (35) Bushin, L. B.; Seyedsayamdost, M. R. Guidelines for Determining the Structures of Radical SAM Enzyme-Catalyzed Modifications in the Biosynthesis of RiPP Natural Products. *Methods Enzymol.* **2018**, *606*, 439–460.
- (36) Benjdia, A.; Guillot, A.; Ruffié, P.; Leprince, J.; Berteau, O. Post-translational Modification of Ribosomally Synthesized Peptides by a Radical SAM Epimerase in *Bacillus subtilis*. *Nat. Chem.* **2017**, *9*, 698–707.
- (37) Parent, A.; Benjdia, A.; Guillot, A.; Kubiak, X.; Balty, C.; Lefranc, B.; Leprince, J.; Berteau, O. Mechanistic Investigations of PoyD, a Radical S-Adenosyl-l-methionine Enzyme Catalyzing Iterative and Directional Epimerizations in Polytheonamide A Biosynthesis. *J. Am. Chem. Soc.* 2018, 140, 2469–2477.
- (38) Besandre, R. A.; Chen, Z.; Davis, I.; Zhang, J.; Ruszczycky, M. W.; Liu, A.; Liu, H. W. HygY Is a Twitch Radical SAM Epimerase with Latent Dehydrogenase Activity Revealed upon Mutation of a Single Cysteine Residue. *J. Am. Chem. Soc.* **2021**, *143*, 15152–15158.
- (39) Taylor, S. V.; Kelleher, N. L.; Kinsland, C.; Chiu, H. J.; Costello, C. A.; Backstrom, A. D.; McLafferty, F. W.; Begley, T. P. Thiamin Biosynthesis in *Escherichia coli*. Identification of ThiS Thiocarboxylate as the Immediate Sulfur Donor in the Thiazole Formation. *J. Biol. Chem.* 1998, 273, 16555–16560.
- (40) Xi, J.; Ge, Y.; Kinsland, C.; McLafferty, F. W.; Begley, T. P. Biosynthesis of the Thiazole Moiety of Thiamin in *Escherichia coli*: Identification of an Acyldisulfide-Linked Protein Protein Conjugate That Is Functionally Analogous to the Ubiquitin/E1 Complex. *Proc. Natl. Acad. Sci. U.S.A.* **2001**, *98*, 8513–8518.
- (41) Butcher, B. G.; Lin, Y. P.; Helmann, J. D. The *yydFGHIJ* Operon of *Bacillus subtilis* Encodes a Peptide that Induces the LiaRS Two-component System. *J. Bacteriol.* **2007**, *189*, 8616–8625.
- (42) Freeman, M. F.; Gurgui, C.; Helf, M. J.; Morinaka, B. I.; Uria, A. R.; Oldham, N. J.; Sahl, H. G.; Matsunaga, S.; Piel, J. Metagenome Mining Reveals Polytheonamides as Posttranslationally Modified Ribosomal Peptides. *Science* **2012**, *338*, 387–390.
- (43) Morinaka, B. I.; Vagstad, A. L.; Helf, M. J.; Gugger, M.; Kegler, C.; Freeman, M. F.; Bode, H. B.; Piel, J. Radical S-adenosyl methionine epimerases: regioselective introduction of diverse D-amino acid patterns into peptide natural products. *Angew. Chem., Int. Ed. Engl.* **2014**, *53*, 8503–8507.
- (44) Fuchs, S. W.; Lackner, G.; Morinaka, B. I.; Morishita, Y.; Asai, T.; Riniker, S.; Piel, J. A Lanthipeptide-like N-Terminal Leader Region Guides Peptide Epimerization by Radical SAM Epimerases:

- Implications for RiPP Evolution. Angew. Chem., Int. Ed. Engl. 2016, 55, 12330–12333.
- (45) Freeman, M. F.; Helf, M. J.; Bhushan, A.; Morinaka, B. I.; Piel, J. Seven Enzymes Create Extraordinary Molecular Complexity in an Uncultivated Bacterium. *Nat. Chem.* **2017**, *9*, 387–395.
- (46) Morinaka, B. I.; Verest, M.; Freeman, M. F.; Gugger, M.; Piel, J. An Orthogonal D₂O-Based Induction System that Provides Insights into D-Amino Acid Pattern Formation by Radical S-Adenosylmethionine Peptide Epimerases. *Angew. Chem., Int. Ed. Engl.* **2017**, *56*, 762–766.
- (47) Vagstad, A. L.; Kuranaga, T.; Püntener, S.; Pattabiraman, V. R.; Bode, J. W.; Piel, J. Introduction of d-Amino Acids in Minimalistic Peptide Substrates by an S-Adenosyl-l-Methionine Radical Epimerase. *Angew. Chem., Int. Ed. Engl.* **2019**, *58*, 2246–2250.
- (48) Benjdia, A.; Berteau, O. Radical SAM Enzymes and Ribosomally-Synthesized and Post-Translationally Modified Peptides: A Growing Importance in the Microbiomes. *Front. Chem.* **2021**, *9*, No. 678068.
- (49) Hamada, T.; Matsunaga, S.; Yano, G.; Fusetani, N. Polytheonamides A and B, highly cytotoxic, linear polypeptides with unprecedented structural features, from the marine sponge, *Theonella swinhoei*. J. Am. Chem. Soc. 2005, 127, 110–118.
- (50) Hamada, T.; Matsunaga, S.; Fujiwara, M.; Fujita, K.; Hirota, H.; Schmucki, R.; Güntert, P.; Fusetani, N. Solution structure of polytheonamide B, a highly cytotoxic nonribosomal polypeptide from marine sponge. *J. Am. Chem. Soc.* **2010**, *132*, 12941–12945.
- (51) Walsh, C. T. Blurring the Lines between Ribosomal and Nonribosomal Peptide Scaffolds. ACS Chem. Biol. 2014, 9, 1653—1661.
- (52) Claesen, J.; Bibb, M. Genome Mining and Genetic Analysis of Cypemycin Biosynthesis Reveal an Unusual Class of Posttranslationally Modified Peptides. *Proc. Natl. Acad. Sci. U.S.A.* **2010**, *107*, 16297–16302.
- (53) Ma, S.; Zhang, Q. Linaridin Natural Products. *Nat. Prod. Rep.* **2020**, 37, 1152–1163.
- (54) Xue, Y.; Wang, X.; Liu, W. Reconstitution of the Linaridin Pathway Provides Access to the Family-Determining Activity of Two Membrane-Associated Proteins in the Formation of Structurally Underestimated Cypemycin. J. Am. Chem. Soc. 2023, 145, 7040—7047.
- (55) Shang, Z.; Winter, J. M.; Kauffman, C. A.; Yang, I.; Fenical, W. Salinipeptins: Integrated Genomic and Chemical Approaches Reveal Unusual d-Amino Acid-Containing Ribosomally Synthesized and Post-Translationally Modified Peptides (RiPPs) from a Great Salt Lake Streptomyces sp. ACS Chem. Biol. 2019, 14, 415–425.
- (56) Xiao, W.; Satoh, Y.; Ogasawara, Y.; Dairi, T. Biosynthetic Gene Cluster of Linaridin Peptides Contains Epimerase Gene. *Chem-BioChem* **2022**, 23, No. e202100705.
- (57) Chu, L.; Cheng, J.; Zhou, C.; Mo, T.; Ji, X.; Zhu, T.; Chen, J.; Ma, S.; Gao, J.; Zhang, Q. Hijacking a Linaridin Biosynthetic Intermediate for Lanthipeptide Production. *ACS Chem. Biol.* **2022**, *17*, 3198–3206.
- (58) Hou, J.; Robbel, L.; Marahiel, M. A. Identification and Characterization of the Lysobactin Biosynthetic Gene Cluster Reveals Mechanistic Insights into an Unusual Termination Module Architecture. *Chem. Biol.* **2011**, *18*, 655–664.
- (59) Schafhauser, T.; Jahn, L.; Kirchner, N.; Kulik, A.; Flor, L.; Lang, A.; Caradec, T.; Fewer, D. P.; Sivonen, K.; van Berkel, W. J. H.; et al. Antitumor Astins Originate from the Fungal Endophyte *Cyanodermella asteris* Living within the Medicinal Plant *Aster tataricus*. *Proc. Natl. Acad. Sci. U.S.A.* **2019**, *116*, 26909–26917.
- (60) Oves-Costales, D.; Gren, T.; Sterndorff, E. B.; Martín, J.; Ortiz-López, F. J.; Jørgensen, T. S.; Jiang, X.; Román-Hurtado, F.; Reyes, F.; Genilloud, O.; Weber, T. Identification and Heterologous Expression of the Globomycin Biosynthetic Gene Cluster. *Synth. Syst. Biotechnol.* **2023**, *8*, 206–221.
- (61) Hochstrasser, M. Origin and Function of Ubiquitin-like Proteins. *Nature* **2009**, 458, 422–429.

- (62) Ghodge, S. V.; Biernat, K. A.; Bassett, S. J.; Redinbo, M. R.; Bowers, A. A. Post-Translational Claisen Condensation and Decarboxylation En Route to the Bicyclic Core of Pantocin A. J. Am. Chem. Soc. 2016, 138, 5487–5490.
- (63) Zimmermann, L.; Stephens, A.; Nam, S.-Z.; Rau, D.; Kübler, J.; Lozajic, M.; Gabler, F.; Söding, J.; Lupas, A. N.; Alva, V. A Completely Reimplemented MPI Bioinformatics Toolkit with a New HHpred Server at Its Core. *J. Mol. Biol.* **2018**, *430*, 2237–2243.
- (64) Ji, G.; Beavis, R.; Novick, R. P. Bacterial Interference Caused by Autoinducing Peptide Variants. *Science* **1997**, *276*, 2027–2030.
- (65) Wang, B.; Zhao, A.; Novick, R. P.; Muir, T. W. Key Driving Forces in the Biosynthesis of Autoinducing Peptides Required for Staphylococcal Virulence. *Proc. Natl. Acad. Sci. U.S.A.* **2015**, *112*, 10679–10684.
- (66) Verbeke, F.; De Craemer, S.; Debunne, N.; Janssens, Y.; Wynendaele, E.; Van de Wiele, C.; De Spiegeleer, B. Peptides as Quorum Sensing Molecules: Measurement Techniques and Obtained Levels in vitro and in vivo. Front. Neurosci. 2017, 11, 183.
- (67) Repka, L. M.; Chekan, J. R.; Nair, S. K.; van der Donk, W. A. Mechanistic Understanding of Lanthipeptide Biosynthetic Enzymes. *Chem. Rev.* **2017**, *117*, 5457–5520.
- (68) Khaliullin, B.; Aggarwal, P.; Bubas, M.; Eaton, G. R.; Eaton, S. S.; Latham, J. A. Mycofactocin Biosynthesis: Modification of the Peptide MftA by the Radical S-Adenosylmethionine Protein MftC. *FEBS Lett.* **2016**, *590*, 2538–2548.
- (69) Ayikpoe, R.; Ngendahimana, T.; Langton, M.; Bonitatibus, S.; Walker, L. M.; Eaton, S. S.; Eaton, G. R.; Pandelia, M. E.; Elliott, S. J.; Latham, J. A. Spectroscopic and Electrochemical Characterization of the Mycofactocin Biosynthetic Protein, MftC, Provides Insight into Its Redox Flipping Mechanism. *Biochemistry* **2019**, *58*, 940–950.
- (70) Flühe, L.; Knappe, T. A.; Gattner, M. J.; Schäfer, A.; Burghaus, O.; Linne, U.; Marahiel, M. A. The Radical SAM Enzyme AlbA Catalyzes Thioether Bond Formation in Subtilosin A. *Nat. Chem. Biol.* **2012**, *8*, 350–357.
- (71) Flühe, L.; Burghaus, O.; Wieckowski, B. M.; Giessen, T. W.; Linne, U.; Marahiel, M. A. Two [4Fe-4S] Clusters Containing Radical SAM Enzyme SkfB Catalyze Thioether Bond Formation During the Maturation of the Sporulation Killing Factor. *J. Am. Chem. Soc.* **2013**, 135, 959–962.
- (72) Kincannon, W. M.; Bruender, N. A.; Bandarian, V. A Radical Clock Probe Uncouples H-Atom Abstraction from Thioether Cross-Link Formation by the Radical S-Adenosyl-L-Methionine Enzyme SkfB. *Biochemistry* **2018**, *57*, 4816–4823.
- (73) Lewis, J. K.; Jochimsen, A. S.; Lefave, S. J.; Young, A. P.; Kincannon, W. M.; Roberts, A. G.; Kieber-Emmons, M. T.; Bandarian, V. New Role for Radical SAM Enzymes in the Biosynthesis of Thio(Seleno)Oxazole RiPP Natural Products. *Biochemistry* **2021**, 60, 3347–3361.
- (74) Barr, I.; Latham, J. A.; Iavarone, A. T.; Chantarojsiri, T.; Hwang, J. D.; Klinman, J. P. Demonstration That the Radical S-Adenosylmethionine (SAM) Enzyme PqqE Catalyzes de Novo Carbon-Carbon Cross-linking within a Peptide Substrate PqqA in the Presence of the Peptide Chaperone PqqD. *J. Biol. Chem.* **2016**, 291, 8877–8884.
- (75) Hudson, G. A.; Burkhart, B. J.; DiCaprio, A. J.; Schwalen, C. J.; Kille, B.; Pogorelov, T. V.; Mitchell, D. A. Bioinformatic Mapping of Radical S-Adenosylmethionine-Dependent Ribosomally Synthesized and Post-Translationally Modified Peptides Identifies New $C\alpha$, $C\beta$, and $C\gamma$ -Linked Thioether-Containing Peptides. *J. Am. Chem. Soc.* **2019**, *141*, 8228–8238.
- (76) Nguyen, T. Q. N.; Tooh, Y. W.; Sugiyama, R.; Nguyen, T. P. D.; Purushothaman, M.; Leow, L. C.; Hanif, K.; Yong, R. H. S.; Agatha, I.; Winnerdy, F. R.; Gugger, M.; Phan, A. T.; Morinaka, B. I. Post-Translational Formation of Strained Cyclophanes in Bacteria. *Nat. Chem.* **2020**, *12*, 1042–1053.
- (77) Sugiyama, R.; Suarez, A. F. L.; Morishita, Y.; Nguyen, T. Q. N.; Tooh, Y. W.; Roslan, M. N. H. B.; Lo Choy, J.; Su, Q.; Goh, W. Y.; Gunawan, G. A.; Wong, F. T.; Morinaka, B. I. The Biosynthetic Landscape of Triceptides Reveals Radical SAM Enzymes That

- Catalyze Cyclophane Formation on Tyr- and His-Containing Motifs. *J. Am. Chem. Soc.* **2022**, *144*, 11580–11593.
- (78) Nguyen, H.; Made Kresna, I. D.; Böhringer, N.; Ruel, J.; Mora, E.; Kramer, J. C.; Lewis, K.; Nicolet, Y.; Schäberle, T. F.; Yokoyama, K. Characterization of a Radical SAM Oxygenase for the Ether Crosslinking in Darobactin Biosynthesis. *J. Am. Chem. Soc.* **2022**, *144*, 18876–18886.
- (79) Yokoyama, K.; Lilla, E. A. C-C Bond Forming Radical SAM Enzymes Involved in the Construction of Carbon Skeletons of Cofactors and Natural Products. *Nat. Prod. Rep.* **2018**, *35*, *660*–694. (80) Guo, S.; Wang, S.; Ma, S.; Deng, Z.; Ding, W.; Zhang, Q. Radical SAM-dependent Ether Crosslink in Daropeptide Biosynthesis. *Nat. Commun.* **2022**, *13*, 2361.
- (81) Zhang, Y.; Min, S.; Sun, Y.; Ye, J.; Zhou, Z.; Li, H. Characteristics of Population Structure, Antimicrobial Resistance, Virulence Factors, and Morphology of Methicillin-Resistant *Macrococcus caseolyticus* in Global Clades. *BMC Microbiol.* **2022**, 22, 266.